

Document downloaded from:

<http://hdl.handle.net/10251/59817>

This paper must be cited as:

Galindo, J.; Tiseira Izaguirre, AO.; Fajardo, P.; Navarro García, R. (2013). Analysis of the influence of different real flow effects on computational fluid dynamics boundary conditions based on the method of characteristics. *Mathematical and Computer Modelling*. 57(7-8):1957-1964. doi:10.1016/j.mcm.2012.01.016.



The final publication is available at

<http://dx.doi.org/10.1016/j.mcm.2012.01.016>

Copyright Elsevier

Additional Information

NOTICE:

this is the author's version of a work that was accepted for publication in *Mathematical and Computer Modelling*. Changes resulting from the publishing process, such as peer review, editing, corrections, structural formatting, and other quality control mechanisms may not be reflected in this document. Changes may have been made to this work since it was submitted for publication. A definitive version was subsequently published as:

J. Galindo, A. Tiseira, P. Fajardo, R. Navarro, Analysis of the influence of different real flow effects on computational fluid dynamics boundary conditions based on the method of characteristics, *Mathematical and Computer Modelling* 57 (7-8) (2013) 1957-1964. [doi:10.1016/j.mcm.2012.01.016](https://doi.org/10.1016/j.mcm.2012.01.016)

Analysis of the Influence of Different Real Flow Effects on CFD Boundary Conditions Based on the MoC

J. Galindo, A. Tiseira, P. Fajardo and R. Navarro

*CMT - Motores Térmicos,
Universidad Politécnica de Valencia,
Camino de Vera S/N, 46022 Valencia*

Abstract

Nowadays, turbocharged internal combustion engines (ICEs) are very common in automotive powerplants, monopolizing the Diesel sector and having a steadily increasing percentage in the gasoline one. In this frame, the interest in modeling the behavior of the turbomachinery components involved, with the ultimate goal of characterizing the performance of the turbocharged ICE, seems clear. A turbomachine can be simulated using 3D-CFD software, but its computational cost does not allow to reproduce the whole turbocharger test rig. Moreover, the existence of long ducts requires a considerable computational time until the pressure reflections at the boundaries dissipate in order to reach a periodic solution.

The use of non-reflecting boundary conditions reduces the needed length of ducts without introducing spurious wave reflections. An anechoic boundary condition (BC) based on the Method of Characteristics has been previously developed, considering the case of an inviscid and adiabatic 1D flow of a perfect gas. However, real flows do not behave in such ideal manner. In this paper, the extension of the scope of the previous BC is sought. In this way, a methodology to evaluate the performance of the anechoic BC under these real flow situations is shown. The consideration of ideal gas instead of perfect gas, the flow viscosity and the non-homentropic flow makes it necessary to modify the Method of Characteristics, since the Riemann Invariants are not constant any more. In this frame they are referred to as Riemann Variables. An additional issue that has been considered is the effect of swirl flow, as the one in the turbine outlet, on the anechoic BC. Some improvements to be implemented in the BC are proposed in order to have a better performance in these real flow situations.

Keywords: CFD simulation, CFD BC, Boundary Condition, Real Effects, Anechoic BC, Method of Characteristics

1. Introduction

The current legislation on internal combustion engines (ICEs) sets limits for pollutant and noise emissions that would have seemed unreachable not so long ago. This fact, combined with

Email address: galindo@mot.upv.es, anti1@mot.upv.es, pabfape@mot.upv.es, ronagar1@mot.upv.es (J. Galindo, A. Tiseira, P. Fajardo and R. Navarro)

the necessity to keep production costs bounded, has driven researchers to optimize the efficiency of ICEs. In particular, the improvement of gas exchange processes has been thoroughly investigated [1, 2, 3]. Unfortunately, the effect on an ICE performance due to modifications in gas exchange components cannot be predicted beforehand, since the interactions between the acoustic responses of the different elements involved (intake or exhaust systems, turbomachinery, etc.) are quite strong [4, 5]. In this way, the use of Computational Fluid Dynamics (CFD) has helped researchers in understanding flow behavior inside these components [6, 7] and also allowing to predict the results of different configurations without the cost of testing them experimentally [8]. That is the reason that explains the growing use of CFD for research and development purposes.

Modeling turbomachinery poses particular problems: their geometrical complexity requires the use of viscous compressible 3D codes to capture properly the flow behavior. Additionally a mesh motion procedure is needed in order to truthfully reproduce the rotor flow. However this makes the computational cost even higher. If the objective of the computation is to obtain the acoustic response of a system the use of long ducts is needed in order to avoid interferences with the boundaries. This fact can be easily understood when compared to the experimental procedure used to obtain the acoustic response in an impulse test rig as the one simulated in [6].

Including those long ducts in the computational domain leads to a dramatic increase of the computational cost [9]. In this frame, the idea of developing a non-reflecting boundary condition (NRBC) that behaves as a long duct seems interesting. Since the acoustic response of these long ducts is supposed to be the lack of wave reflection, several researchers [10, 11, 12] have tried to develop the so-called non-reflecting or anechoic boundary conditions (BC), to be able to eliminate these components without any penalty in the accuracy. A similar reasoning can be followed if a turbocharger test rig has to be simulated, in which long ducts are needed in order to have uniform flow at the measurement sections. Their inclusion in the computational domain could represent even doubling the number of cells in some configurations.

In [13], an anechoic BC was developed, which is briefly reviewed in section 2. However, it assumes the existence of an 1D inviscid and adiabatic flow of a perfect gas. Since it is intended to be used in a turbomachinery outlet, these constraints could affect the BC performance. In this paper, three different real flow effects will be studied: non-perfect gas, viscous flow and swirling flow. In sections 3-5, these effects will be reviewed, their influence on the anechoic BC will be analyzed and an implementation improvement (where available) will be proposed. Finally, in section 6, the main conclusions of the work will be presented.

2. 1D Anechoic BC

The current analysis is going to be performed in an anechoic BC which has been previously developed in [13]. An anechoic end is an outlet BC in which information does not travel upstream of the boundary condition (anechoic means literally without echo). This non-reflecting BC should thus behave as a long duct, allowing to save computational cost.

If the assumption of 1D inviscid flow of a perfect gas with negligible heat transfer is made, the evolution of the flow can be described by means of the Method of Characteristics (MoC). The MoC identifies the information traveling upstream with the Riemann invariant β . In order to mimic the anechoic behavior an infinite duct is considered. The notation used hereinafter is presented in figure 1. It is known that when non-homentropic flow is considered the Riemann invariants cease being constant. Therefore they are renamed as Riemann variables. Modifications of the Riemann variables can be found in the literature [14, 15]. In figure 1 the values of the Riemann variables reaching the boundary, in this case β_{in} , are shown. If the characteristic line is

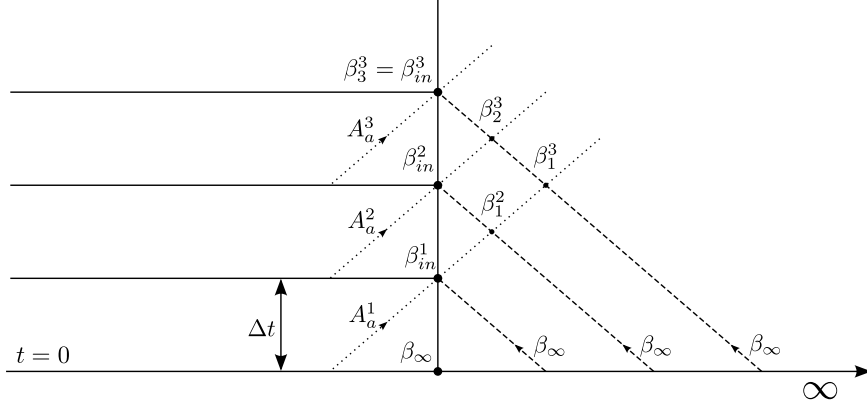


Figure 2: Modification of the β values due to the changes of entropy that occur at the crossing points of the two characteristic lines.

3. Non-Perfect Gas

The MoC was originally developed under the hypothesis of perfect gas [17]. However, if an ideal (but not calorically perfect) gas is considered, the MoC can still be used with some modifications. Following [14], if $c_p = f(T)$, the following variables replace the Riemann variables:

$$\begin{aligned}
 \lambda' &= \int_{T_{ref}}^T \sqrt{\frac{c_p c_v}{RT}} dT + u \\
 \beta' &= \int_{T_{ref}}^T \sqrt{\frac{c_p c_v}{RT}} dT - u \\
 s &= \int_{T_{ref}}^T \frac{q + uG}{T} dT
 \end{aligned} \tag{2}$$

The polynomial law stated in [18] or the polynomial function used in ANSYS-FLUENT [19] was used for $c_p(T)$. Following a similar criterion, the first term of the Riemann variables as defined in (2) can be expressed as a polynomial of temperature.

The methodology used to impose the boundary condition is the same as the one used in [13]: the fluid variables at the boundary will be recovered from the Riemann variables reaching it. The only difference is that the equations are now non-linear. From the values of λ' and β' reaching the boundary, it is possible to obtain the value of the flow velocity and a polynomial of temperature. It is necessary to find the roots of the polynomial in order to obtain the temperature. In order to solve this problem a Newton-Raphson scheme was used to find the value of temperature from the Riemann variables at every time step. Additionally, Horner's algorithm was used in order to efficiently evaluate polynomial expressions. Finally, the value of the pressure at the boundary was obtained from the entropy and the previously calculated temperature.

The last thing that it is worth to mention when dealing with a non-perfect gas is that the value of the modifier due to changes in entropy used in [13] will not remain the same. The new formulation can be obtained from [14] and it establishes that:

$$d\beta'|_s = \sqrt{\frac{c_v T}{c_p R}} ds \quad (3)$$

The application of this new formulation of the modifier due to variations of entropy to the Anechoic BD scheme is straightforward.

To check the influence of this behavior, a simulation was run in which a pressure pulse is applied to a non-calorically perfect gas. In the left side of figures 3 and 4, one can see how the former Riemann variables A_a and β vary when λ arrives. When the new formulation is implemented, these changes disappear, as can be seen in the right side of figures 3 and 4.

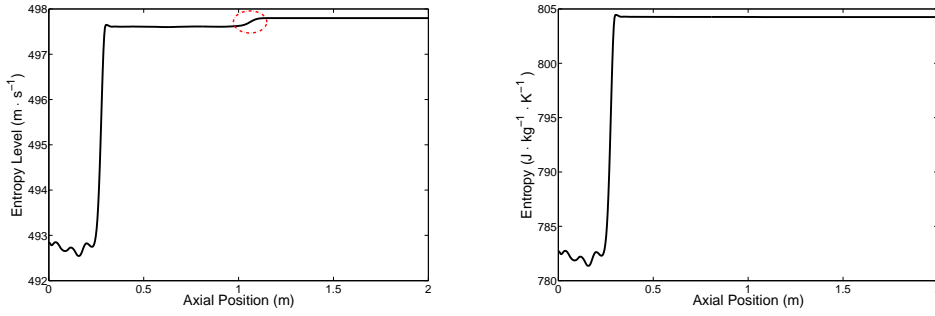


Figure 3: Distribution of A_a (left side) and s (right side) in the axis of the duct after 800 time-steps

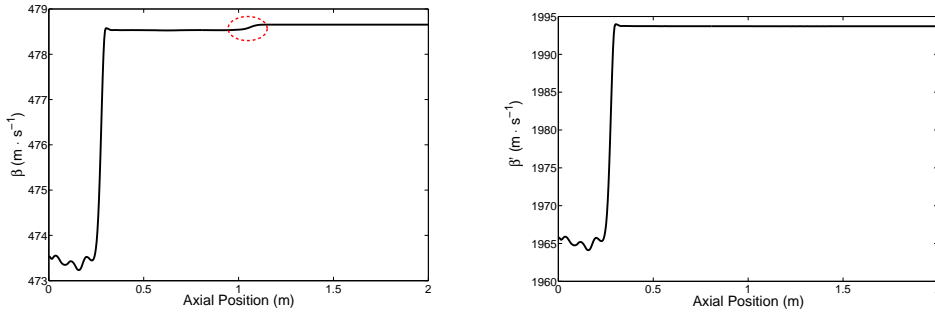


Figure 4: Distribution of β (left side) and β' (right side) in the axis of the duct after 800 time-steps

4. Viscous Flow

The existence of viscosity in the flow has various effects introducing further complexity in the anechoic BC. First, the diffusive transport induced by viscosity cannot be modeled by the MoC, since it only deals with the hyperbolic part of the Navier-Stokes equations (i.e, the Euler equations). However, since the Reynolds number in the intended applications (flow in ICEs) is high ($Re_D \approx 2 \cdot 10^5$ for the considered case), the diffusive transport should be negligible compared

to the convection terms. Moreover, there is a loss in momentum due to the existence of friction. This effect is mainly concentrated in the surroundings of the wall. This effect decreases with smoother ducts and higher Reynolds number (until fully developed turbulent flow is reached). Anyway, as it has been exposed before, there exists a modifier that takes into account this effect in the value of each Riemann variable along its respective characteristic line:

$$d\beta|_f = -(\gamma - 1) \left[1 - (\gamma - 1) \frac{u}{a} \right] \frac{f}{D} u^2 \frac{u}{|u|} dt \quad (4)$$

In (4), f is the Fanning friction factor, defined as $f = \frac{\tau_w}{\frac{1}{2}\rho u^2}$. In this work, f was estimated by means of the explicit Swamee-Jain equation:

$$f = \frac{0.0625}{\left(\log_{10} \left(\frac{\epsilon}{3.7D} + \frac{5.74}{Re^{0.9}} \right) \right)^2} \quad (5)$$

It should be pointed out that eq. (5) should not be confused with the more common Swamee-Jain equation for the Darcy friction factor, which is 4 times larger than Fanning's one. It should be mentioned that all the variables needed to evaluate eq. (5) are taken from the previous time-step, in order to keep the expression being explicit.

Besides the previous two effects, friction has another effect that is relevant not because of the use of the MoC but due to the anechoic BC approach. In its development, it was stated that, for inviscid flows, β only had to take into account the entropy changes. However, in viscous flows, when a λ -wave (C^+) arrives, velocity raises, thus increasing the friction effect and therefore changing the values of the Riemann variables. In order to clarify this fact, a simulation of a long duct with a isentropic step pressure pulse at the inlet of the duct was performed. The evolution of flow velocity and β were monitorized at a given section, which in the case presented in figure 5 is the section at $0.9m$ from the inlet. If viscosity were not taken into account, the velocity would increase once the pulse reaches the considered section and afterwards it would remain constant. However, if viscosity were considered, the flow velocity would continue decreasing after the λ -wave had passed as it is shown in 5(a). When a wave reaches the BC, the change of β that still happens at the virtual duct at the right of the boundary condition is sent backwards. This last fact makes the former anechoic approach invalid to correctly model the acoustic response of an infinite duct with friction, because that duct produces reflections.

Therefore, since the information created at the right of the BC must be taken into account, one should model it, and a 1D-3D coupled simulation such as described in [9] could be helpful. Using this approach would allow to model the response of a sufficiently long duct but reducing at the same time the computational cost when compared to a fully 3D simulation. It is worth considering how long the duct should be for this approach to be useful. It is well known that in the frictional flow inside a duct the flow velocity increases along the duct. Therefore it will reach a point in which the flow will choke and will pass to supersonic regime. After passing to supersonic, it is obvious that no information will travel upstream. The only thing that has to be considered is that this point will change with the flow conditions.

Despite the previous comments, one could want to use the developed anechoic BC with viscous flow, if the reduction of computational time was supposed to compensate the loss of accuracy. Thus, a simulation was performed comparing the behavior of a long duct and a short one with the anechoic BC in a turbulent flow, as shown in 6(a). The comparison between this simulation and the corresponding long duct is shown in figure 6(b).

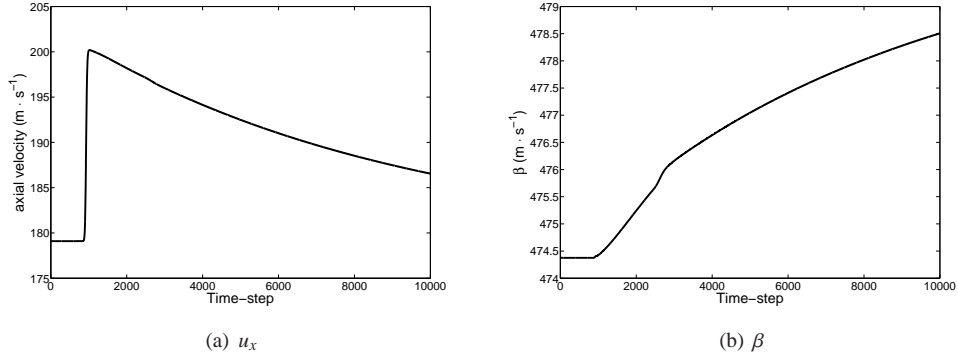
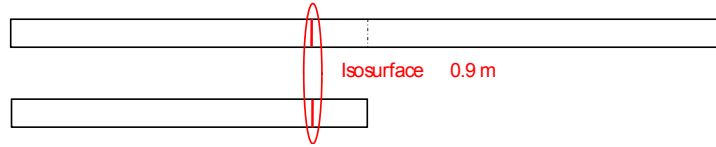
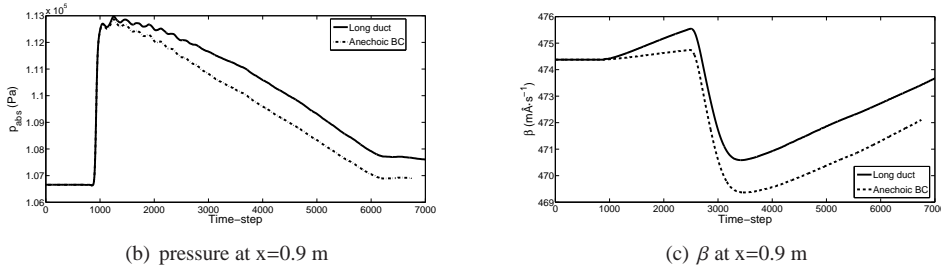


Figure 5: Evolution with time in a given section of u_x (a) and β (b)



(a) Computational domains



(b) pressure at $x=0.9$ m

(c) β at $x=0.9$ m

Figure 6: Computational domains used to evaluate the behavior of the Anechoic BC (a) and the evolution of pressure (b) and β (c) in both ducts

5. Swirling Flow

As already commented, among other applications, the anechoic BC is intended to be used as the outlet boundary in a turbine simulation. However, the flow downstream of a turbine is no longer 1D, because of the swirl created by the impeller. This swirl is even more important when dealing with off-design points. One of the main problems when using CFD commercial codes is that the BCs available are mainly uniform flow BC. This is normally not a serious issue if the main interest of the computation lies far from the boundary. However, in the case of the development of new BC, and particularly with the anechoic BC, is necessary to reproduce the flow behavior close to the boundary. Therefore, a different approach must be followed in order to use the anechoic BC.

If the radial velocity is neglected, a swirling flow is said to be in radial equilibrium ([20]). In such flows, the pressure radial profile satisfies the following equation:

$$\frac{dp}{dr} = \rho(r) \frac{v_{\theta}^2(r)}{r} = F(r) \quad (6)$$

Thus, if radial equilibrium is supposed to be achieved at every time-step, one can obtain the pressure profile at the BC at a certain time-step provided that the pressure at the axis (p_{axis}), in order to obtain the integration constant, and the $F(r)$ profile are known.

Regarding the value of p_{axis} , it can be assumed that the MoC can be still applied to the axis, because $v_{rad} = 0$ due to axial symmetry, and therefore the axis could be assumed to be 1D. On the other side, $F(r)$ is approximated by its value at the previous time-step. This explicit approach is used to avoid the iterative process otherwise required to define all the variables at the BC. Therefore, the pressure profile at the BC is computed integrating eq. (6) between neighbor faces at the BC in increasing radial position, in order to minimize the error, as:

$$p(r, t) = p(r - \Delta r, t) + F(r, t - \Delta T) \cdot \Delta r \quad (7)$$

The integration process is started with the known value of $p(r = 0) = p_{axis}$ obtained by the application of the MoC to the 1D flow of the axis.

The hypothesis of radial equilibrium was checked by running two axisymmetric simulations with a swirling inlet BC: a long duct and a short one with the anechoic BC with radial equilibrium. $p(r)$ profiles of both ducts at the section at 1m (outlet of the short duct) are compared in fig. 7. It is shown that the pressure profile is correctly obtained with the radial equilibrium approach.

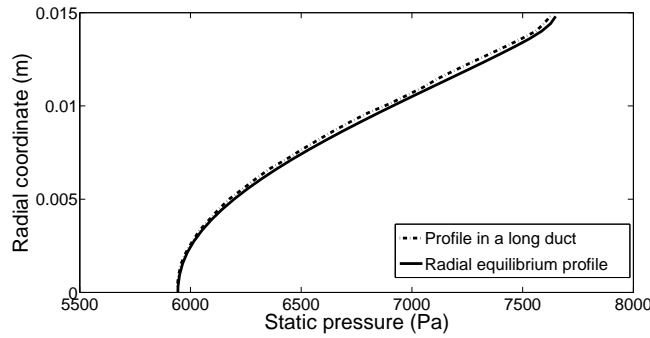


Figure 7: Pressure profile at BC in a long duct (stipped line) compared with the pressure profile obtained imposing radial equilibrium (continuous line)

Then, a transient simulation was run in which a step pressure pulse was set at the inlet of the duct. A comparison between data at section at 0.9m of a long duct and a short one with the anechoic BC was made. The evolution of pressure at the axis is presented in figure 8. As expected, the MoC can be satisfactorily applied to the axis.

Regarding the use of the radial equilibrium to obtain $p(r)$ profile at every time-step, an area-weighted average of pressure at section at 0.9m is provided in figure 9. Good agreement is found between the values obtained by both simulations.

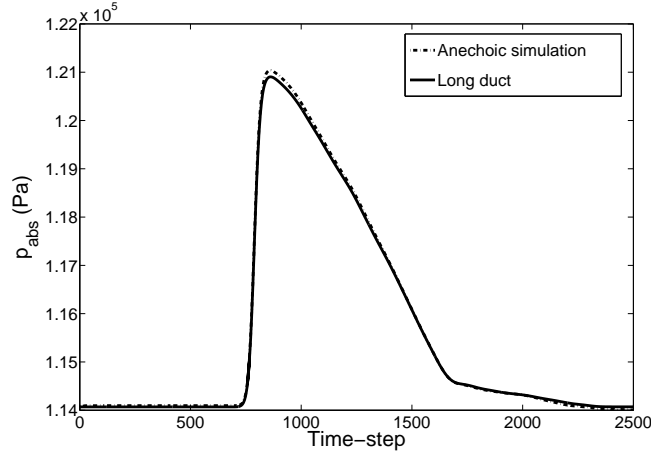


Figure 8: Evolution of pressure at the axis of a long duct and a short duct using the anechoic BC

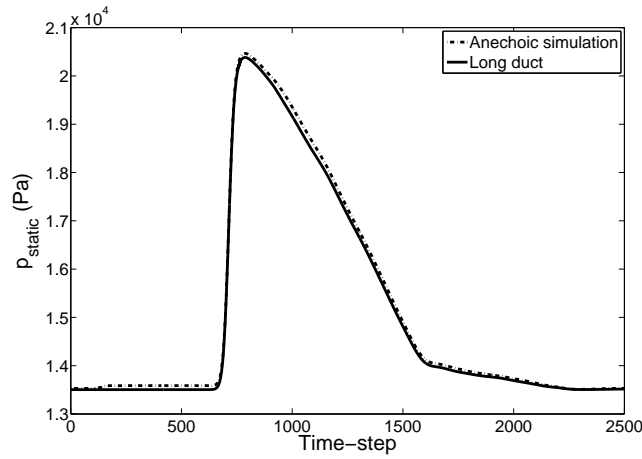


Figure 9: Evolution of an area-weighted average of pressure at section at $0.9m$ of a long duct and a short duct using the anechoic BC

6. Conclusions

In a previous work [13], an anechoic BC was developed, based on the assumption of 1D inviscid and adiabatic flow of a perfect gas. In order to be able to use this anechoic BC in a turbomachinery outlet, three different real flow behaviors have been studied in this paper. In section 3, the hypothesis of ideal instead of perfect gas has been reviewed. A solution has been proposed, and it has been shown to improve significantly the performance of the non-reflecting BC. Then, in section 4, the implications of dealing with viscous flow have been investigated. The effect of wall friction has been incorporated into the BC by means of a proper modifier of the Riemann variables and the use of a correlation for the friction factor. It has been shown that

an infinite duct does send information backwards when receiving an incoming pressure wave. Therefore, the anechoic approach would never be able to reproduce reliably the behavior of a long duct. However, the anechoic BC could still be used to reduce the time to achieve convergence due to the absence of reflections, but taking into account the lack of accuracy regarding the simulation of the whole duct. Finally, in section 5, the existence of swirl (characteristic of a turbine's outlet) has been analyzed. An approach to obtain the whole pressure profile at the outlet has been developed, assuming that the flow is in radial equilibrium. Although the analysis has been carried out for an anechoic BC, similar conclusions could be established for any other BC developed by means of the MoC.

List of Symbols

a	speed of sound	$m \cdot s^{-1}$
C	Characteristic line	–
c_p	specific heat capacity at constant pressure	$J \cdot kg^{-1} \cdot K^{-1}$
c_v	specific heat capacity at constant volume	$J \cdot kg^{-1} \cdot K^{-1}$
D	hydraulic diameter	m
f	friction coefficient	–
G	specific momentum loss due to friction	$m \cdot s^{-2}$
p	pressure	Pa
q	specific heat transfer rate	$W \cdot kg^{-1}$
r	radial coordinate	m
R	specific gas constant	$J \cdot kg^{-1} \cdot K^{-1}$
Re_D	Reynolds number based on D	–
t	time	s
T	temperature	K
u	velocity in x-direction	$m \cdot s^{-1}$
v_θ	tangential velocity	$m \cdot s^{-1}$
x	coordinate in dominant direction	m
β	backward Riemann Invariant	$m \cdot s^{-1}$
λ	forward Riemann Invariant	$m \cdot s^{-1}$
A_a	entropy level	$m \cdot s^{-1}$
Δt	time-step	s
ϵ	roughness height	m
γ	ratio of specific heats	–
ρ	density	$kg \cdot m^{-3}$
τ_w	wall shear stress	Pa

Sub- and Superscripts

+	forward
–	backward
0	flow
∞	value at infinity
<i>in</i>	reaching the BC
<i>f</i>	friction
<i>N</i>	value at N^{th} time-step
<i>ref</i>	reference

List of abbreviations

1D	one dimensional
3D	three dimensional
BC	boundary condition
CFD	computational fluid dynamics
ICE	internal combustion engine
MoC	Method of Characteristics
NRBC	non-reflecting boundary condition

- [1] J. R. Serrano, F. J. Arnau, P. Piqueras, A. Onorati, G. Montenegro, 1D gas dynamic modelling of mass conservation in engine duct systems with thermal contact discontinuities, *Mathematical and Computer Modelling* 49 (5-6) (2009) 1078–1088. doi:10.1016/j.mcm.2008.03.015.
- [2] C. D. Copeland, R. Martinez-Botas, M. Seiler, Comparison Between Steady and Unsteady Double-Entry Turbine Performance Using the Quasi-Steady Assumption, *Journal of Turbomachinery* 133 (2011) 031001–1/031001–10.
- [3] M. Tancrez, J. Galindo, C. Guardiola, P. Fajardo, O. Varnier, Turbine adapted maps for turbocharger engine matching, *Experimental Thermal and Fluid Science* 35 (1). doi:10.1016/j.expthermflusci.2010.07.018.
- [4] K. S. Peat, A. J. Torregrosa, A. Broatch, T. Fernández, An investigation into the passive acoustic effect of the turbine in an automotive turbocharger, *Journal of sound and vibration* 295 (1-2) (2006) 60–75.
- [5] M. L. Munjal, *Acoustics of ducts and mufflers with application to exhaust and ventilation system design*, Wiley-Interscience, 1987.
- [6] A. Broatch, X. Margot, A. Gil, F. D. Denia, A CFD Approach to the Computation of the Acoustic Response of Exhaust Mufflers, *Journal of Computational Acoustic* 13 (2) (2005) 301–316. doi:10.1142/S0218396X05002682.
- [7] G. Montenegro, A. Onorati, Modeling of Silencers for IC Engine Intake and Exhaust Systems by Means of an Integrated 1D-multiD Approach, *SAE International Journal of Engines* 1 (1) (2009) 466. doi:10.4271/2008-01-0677.
- [8] N. C. Baines, A meanline prediction method for radial turbine efficiency, in: *6th International Conference on Turbocharging and Air Management Systems*, I Mech E, no. C554-6, Concepts ETI, Inc, Institution of Mechanical Engineers, 1998.
- [9] J. Galindo, A. Tiseira, P. Fajardo, R. Navarro, Coupling methodology of 1D finite difference and 3D finite volume CFD codes based on the Method of Characteristics, *Mathematical and Computer Modelling* 54 (2011) 1738–1746. doi:http://dx.doi.org/10.1016/j.mcm.2010.11.078.
- [10] F. Payri, J. M. Desantes, A. J. Torregrosa, Acoustic boundary condition for unsteady one-dimensional flow calculations, *Journal of Sound and Vibration* 188 (1) (1995) 85–110.
- [11] O. V. Atassi, Nonreflecting boundary conditions for the time-dependent convective wave equation in a duct, *Journal of Computational Physics* 197 (2) (2004) 737–758.
- [12] J. R. Dea, F. X. Giraldo, B. Neta, High-order non-reflecting boundary conditions for the linearized 2-D Euler equations: No mean flow case, *Wave Motion* 46 (3) (2009) 210–220.
- [13] A. J. Torregrosa, P. Fajardo, A. Gil, R. Navarro, Non-reflecting boundary conditions based on the Method of Characteristics for its application in 3D CFD codes, Submitted to *Engineering Applications of Computational Fluid Mechanics*.
- [14] D. E. Winterbone, R. J. Pearson, *Theory of Engine Manifold Design : Wave Action Methods for IC Engines*, John Wiley & Sons, 2000.
- [15] G. Guderley, Nonstationary gas flow in thin pipes of variable cross section, Tech. rep., NASA Technical Memorandum N.1196, Washington (December 1948).
- [16] R. S. Benson, J. H. Horlock, D. E. Winterbone, *The thermodynamics and gas dynamics of internal combustion engines*, Vol. 1, Oxford University Press, 1982.
- [17] R. S. Benson, R. D. Garg, D. Woollatt, A numerical solution of unsteady flow problems, *International Journal of Mechanical Sciences* 6 (1) (1964) 117–144. doi:10.1016/0020-7403(64)90009-8.
- [18] D. R. Stull, JANAF thermochemical tables, Tech. rep., DTIC Document (1971).
- [19] Fluent Inc., *Fluent 6.3 Getting Started Guide* (2006).
- [20] S. L. Dixon, C. Hall, *Fluid mechanics and thermodynamics of turbomachinery*, Butterworth-Heinemann, 2010.